



OPEN Comparative effects of streptozotocin, dehydroepiandrosterone and letrozole with high fat diet on ovarian injury induction and functional impairment

Leyi Yu^{1,2,4,5}, Qingjie Peng^{1,5}, Cunling Ma¹, Jiahui Ouyang¹, Hongru Ma¹, Shuzhe Fan^{1,2}, Miao Sun¹, Huiming Ma¹, Xiaoli Du²✉, Xiangdong Zhu²✉, Guangyong Li³✉ & Rui He^{1,2}✉

This study investigates the mechanisms by which environmental factors affect ovarian function. Environmental toxins and unhealthy lifestyles adversely affect women's health, primarily impair ovarian function. Environmental toxins and unhealthy lifestyles can negatively impact women's health, particularly by impairing ovarian function. Streptozotocin (STZ), dehydroepiandrosterone (DHEA) and letrozole (LET) with high-fat diet (HFD) (only LET was combined with HFD), induced models have been experimentally demonstrated to induce ovarian dysfunction. This investigation aims to elucidate their individual and synergistic effects on ovarian function to inform evidence-based prevention and intervention strategies for ovarian dysfunction. ICR/JCL mice (age 4–5 weeks) were subjected to three distinct pathophysiological modeling approaches to simulate ovarian dysfunction. Multiparametric analysis systematically evaluated physiological changes, glycometabolism function, endocrine parameters, and molecular biology. Experimental outcomes demonstrated that STZ, DHEA and LET with HFD significantly affected mice's metabolic and ovarian functions. Mechanistically, the PI3K/AKT signaling pathway was identified as a critical mediator of ovarian dysfunction. In conclusion, this study systematically compared, for the first time, the individual and synergistic effects of STZ, DHEA and LET with HFD on ovarian function in mice, confirming that these environmental factors induce ovarian dysfunction through metabolic disruption and signal transduction pathway dysregulation. Future research should prioritize elucidating the specific molecular mechanisms by which environmental factors impair ovarian function to establish a scientific foundation for developing targeted intervention strategies.

Keywords Environment, Streptozotocin, DHEA, Letrozole, Ovarian function

In recent years, the impact of environmental toxins and unhealthy lifestyles on female reproductive health has attracted widespread attention. Among them, streptozotocin (STZ), dehydroepiandrosterone (DHEA) and letrozole (LET) with high-fat diet (HFD) (only LET was combined with HFD) have been demonstrated to be strongly correlated with ovarian dysfunction^{1–3}.

¹Key Laboratory of Fertility Preservation and Maintenance of Ministry of Education, School of Basic Medical Sciences, Ningxia Medical University, Yinchuan 750000, China. ²Key Laboratory of Ningxia Minority Medicine Modernization Ministry of Education, School of Traditional Chinese Medicine, Ningxia Medical University, Yinchuan 750000, China. ³Department of Urology, The second hospital of Tianjin Medical University Tianjin Institute of Urology, Tianjin 300211, China. ⁴Dawukou Hospital of the Fifth People's Hospital of Ningxia Hui Autonomous Region, Shizuishan 753000, China. ⁵Leyi Yu and Qingjie Peng contributed equally to this work and considered as first authors. ✉email: dx1710902@163.com; zhuxiangdong33@163.com; guangyongli1979@hotmail.com; ruihe515@163.com

STZ is a glucosamine-nitrosourea compound naturally produced by *Streptomyces achromogenes*, a soil microorganism⁴. As an alkylating agent, STZ shares structural similarities with nitrosourea-based anticancer drugs and has been used in pancreatic cancer therapy. However, it is primarily studied for its diabetogenic effects in experimental models⁵. STZ selectively destroys pancreatic β cells in rodents leading to DNA alkylation and subsequent diabetes induction⁶.

DHEA is an endogenous hormone primarily synthesized in the zona reticularis of the adrenal cortex^{7,8}. DHEA primarily circulates in the blood as its sulfate conjugate, DHEA-S (dehydroepiandrosterone sulfate). Approximately 90% of circulating DHEA-S originates from the zona reticularis of the adrenal cortex, and its serum levels serve as a biomarker for adrenal androgen excess. DHEA-S correlates with 24-h urinary excretion of 17-ketosteroids, reflecting similar clinical relevance in evaluating adrenal steroidogenesis⁹. In addition, DHEA, a precursor to androstenedione and testosterone, is predominantly secreted by the adrenal cortex, with minor contributions from the ovaries and testes^{8,10}. While endogenous production dominates, environmental contamination by DHEA and its metabolites has been documented, primarily via human/animal waste and industrial effluents. Studies have shown that exogenous DHEA supplementation may elevate androgen levels^{11,12} and impair oocyte maturation and ovulation^{3,10,13}. However, DHEA levels in the environment are generally low, and its effects on the environment and human health require further research.

LET is an organic compound primarily utilized as an antitumor agent¹⁴. Although specific usage and emission data are limited in available literature, the widespread therapeutic application of letrozole suggests potential environmental exposure². Furthermore, as an aromatase inhibitor, letrozole exhibits a distinct chemical structure and use, potentially enhancing its detectability in aquatic environments compared to other compounds. Letrozole, a third-generation aromatase inhibitor, increases androgen levels via aromatase inhibition, subsequently impairing ovarian function¹⁵ and contributing to the development of polycystic ovary syndrome (PCOS)¹⁶. High-fat diet (HFD) induces adipose tissue expansion, obesity, and hyperinsulinemia, thereby potentiating the pharmacological effects of letrozole¹⁷. However, comprehensive environmental monitoring data are required to evaluate the precise concentrations, spatial distribution, and ecological impacts of letrozole in natural ecosystems.

In this study, we established the scientific background of how environmental factors (STZ, DHEA and LET with HFD), affect ovarian function. Utilizing our experimental design and preliminary findings, we systematically compared the individual and synergistic effects of STZ, DHEA and LET with HFD, on ovarian function in mice, which represents a novel investigation in this field. We confirmed that these environmental factors induce ovarian dysfunction via disrupting ovarian metabolic homeostasis and key signaling pathways. Through this research, we not only deepen our understanding of the relationship between environmental factors and ovarian health, but also provide potential directions for the prevention and treatment of related diseases.

Materials and methods

Experimental materials

Experimental animals

SPF-grade 4–5-week-old female ICR/JCL mice (body weight 22 ± 3 g) were purchased from the Experimental Animal Center of Ningxia Medical University (Animal License No. SYXK (NING) 2020-0001), and housed in the Experimental Animal Center of Ningxia Medical University. All mice were maintained under controlled environmental conditions (temperature 20–22 °C, relative humidity 60–80%) with a 12-h light/dark cycle. Food and water were provided ad libitum, and all animals underwent a 1-week acclimatization period prior to experiments. The experimental protocol was approved by the Institutional Animal Care and Use Committee (IACUC) of Ningxia Medical University.

Main experimental reagents

High fat diet (60% fat, D12492; RESEARCH DIETS), Letrozole tablets (Jiangsu Hengrui Pharmaceutical Co., LTD.), streptozotocin (STZ, SigmaVetec), Dehydroepiandrosterone (DHEA, Beijing Boao Technology Co., LTD.), Soybean oil for injection (Zhejiang Tianyu Yam Oil Co., LTD., F20060027), DNA/RNA/Protein kit (omega, R673402000C31V007), Goat anti-Rabbit IgG (AB, SANTACRUZ), Anti-PI3K, AKT, p-AKT antibody (Affinity), Rabbit anti- β -Actin (Servicebio), Super high speed non-toxic improved pasteurization dyeing kit (Nanjing Jiancheng Technology Co., LTD.), Mouse testosterone (T), estradiol (E2), sex hormone tuberculosis globulin (SHBG), anti-Muller tube hormone (AMH) kit (ELISA, Quanzhou Jiubang Biotechnology Co., LTD.), Reverse transcription kit (PrimeScript™ RT Master Mix, TaKaRa).

Main experimental instruments and consumables

Blood glucose meter (Roche, Switzerland), Roche blood glucose test strips (Roche, Switzerland), Electrophoresis apparatus/electrophoresis tank/trans-blotting apparatus (Bio-Rad, USA), GelDoc XR chemiluminescence gel imaging system (Bio-Rad Instruments, USA), TissueGnostics quantitative tissue cell analysis system (TissueGnostics, Austria).

Experimental methods

Grouping of mice and establishment of the model

After a 1-week adaptation period, the 36 mice were randomly divided into six groups, with six mice in each group housed in separate cages. They were divided into control group (NCD), streptozotocin 15 mg/kg/day group (STZ-15), streptozotocin 30 mg/kg/day group (STZ-30), streptozotocin 60 mg/kg/day group (STZ-60), dehydroepiandrosterone group (DHEA), letrozole with high-fat diet group (LET + HFD). The NCD group was fed an ordinary diet for 40 days. The STZ-15, STZ-30 and STZ-60 groups were intraperitoneally injected with streptozotocin at 15, 30, or 60 mg/kg/day for five consecutive days, followed by continued feeding with standard diet for an additional 35 days¹⁸; DHEA (6 mg/100 g/day) group was injected subcutaneously with DHEA for

21 days¹³. The LET (1 mg/kg/day) group was fed with letrozole combined with high-fat diet for 21 days¹⁹. The grouping, molding method and modeling process are shown in Table 1 and Fig. 1a.

Determination of estrous cycle by vaginal smear method

Ten days after model induction, vaginal smears were collected continuously for 7 days at 4:00 p.m. each day. A small amount of 0.9% saline solution was aspirated into the vaginal cavity using a Pasteur pipette, and the vaginal secretions were placed on glass slides. The estrous cycle stage was observed under an optical microscope, and the stage was recorded. Representative smears from each group were stained with an ultra-fast-non-toxic modified Pasteur stain kit. Nucleated epithelial cells were stained bluish-green, non-nucleated keratinized squamous cells were stained pink, and white blood cells were stained blue-purple¹⁹.

Oral glucose tolerance test (OGTT)

After modeling, the OGTT experiment was conducted by collecting blood via tail vein. Before the experiment, the mice were fasted for 14–16 h, the initial body weight and initial blood glucose were measured. The amount of glucose solution (3 g/kg) was calculated for each mouse. The mice were administered glucose solution intragastrically. Blood glucose levels were measured at 15, 30, 60, and 120 min following glucose administration. After the experiment, the mice were restored to eat freely, and the changes of blood glucose were measured.

Insulin tolerance test (ITT)

After modeling, ITT experiment was performed by collecting blood via tail vein. Before the experiment, the mice were fasted for 4–6 h. We measured the initial body weight and initial blood glucose, and calculated the insulin dosage of each mouse (1 IU/kg). Insulin was administered to the mice via intraperitoneal injection. Blood glucose was measured at 15, 30, 60 and 120 min post-insulin administration. After the experiment, the mice were returned to eat freely, and the changes of blood glucose were measured.

Blood and ovary collection

Before sampling, the body weight of the mice were recorded. The mice were euthanized via intrabitoneal injection of pentobarbital sodium (3%, 100 mg/kg). Blood was collected via cardiac puncture and centrifuged at 1000×g at 2–8 °C for 10 min within 30 min after collection. The supernatant was then collected and stored at –80 °C to avoid repeated freeze–thaw cycles. Additionally, one ovary was collected for histomorphology experiments, while the other ovary was stored in the refrigerator at –80 °C for molecular biology experiments. Anesthesia or euthanasia were performed using methods consistent with the commonly accepted norms of veterinary best practice.

Analysis of serum hormone concentration

The levels of testosterone (T), estradiol (E2), anti-muller test tube hormone (AMH) and sex hormone binding globulin (SHBG) in the serum were measured according to the instructions of ELISA kits. Absorbance values were measured at 450 nm using a microplate reader (Thermo MULTISKAN GO), and hormone concentrations were calculated.

Ovarian hematoxylin and eosin staining (H&E staining)

After fixing the ovarian tissue in 4% formaldehyde at room temperature for 24 h, the tissue underwent dehydration using varying concentrations of ethanol, embedded in paraffin, and sectioned into 4 μm slices. H&E staining was performed^{19,20}.

The pathological morphological changes in the ovaries were observed under a BX-51 upright fluorescence microscope (OLYMPUS, Japan), and the number of follicles at various stages was counted. According to a previous study²¹, follicles were classified into five stages: primordial, primary, secondary, antral, and atretic follicles. Primordial follicles were surrounded by a single layer of flattened granulosa cells, which are flat and closely packed; primary follicles were surrounded by a single layer of cuboidal granulosa cells, which are cube-shaped and tightly arranged. Secondary follicles had at least two layers of granulosa cells and lacked a follicular cavity, antral follicles contained multiple layers of granulosa cells and a follicular cavity, while atretic follicles were composed of atrophied oocyte cells and abnormal granulosa cells. Primordial follicles were observed at 400× magnification, and primary, secondary, and antral follicles were observed at 200× magnification. To avoid duplicate counting, only follicles with clearly visible oocyte were counted²⁰.

Group	STZ-15	STZ-30	STZ-60	DHEA	LET
Modeling drug	STZ	STZ	STZ	DHEA	LET
Method of administration	Intraperitoneal injection	Intraperitoneal injection	Intraperitoneal injection	Subcutaneous injection	Intragastric administration
Drug dose	15 mg/kg/d	30 mg/kg/d	60 mg/kg/d	9 mg/100 g/day	1 mg/kg/day
Diet	Normal die	Normal diet	Normal diet	Normal diet	High fat diet
Molding cycle (days)	40	40	40	21	21

Table 1. Grouping and molding method.

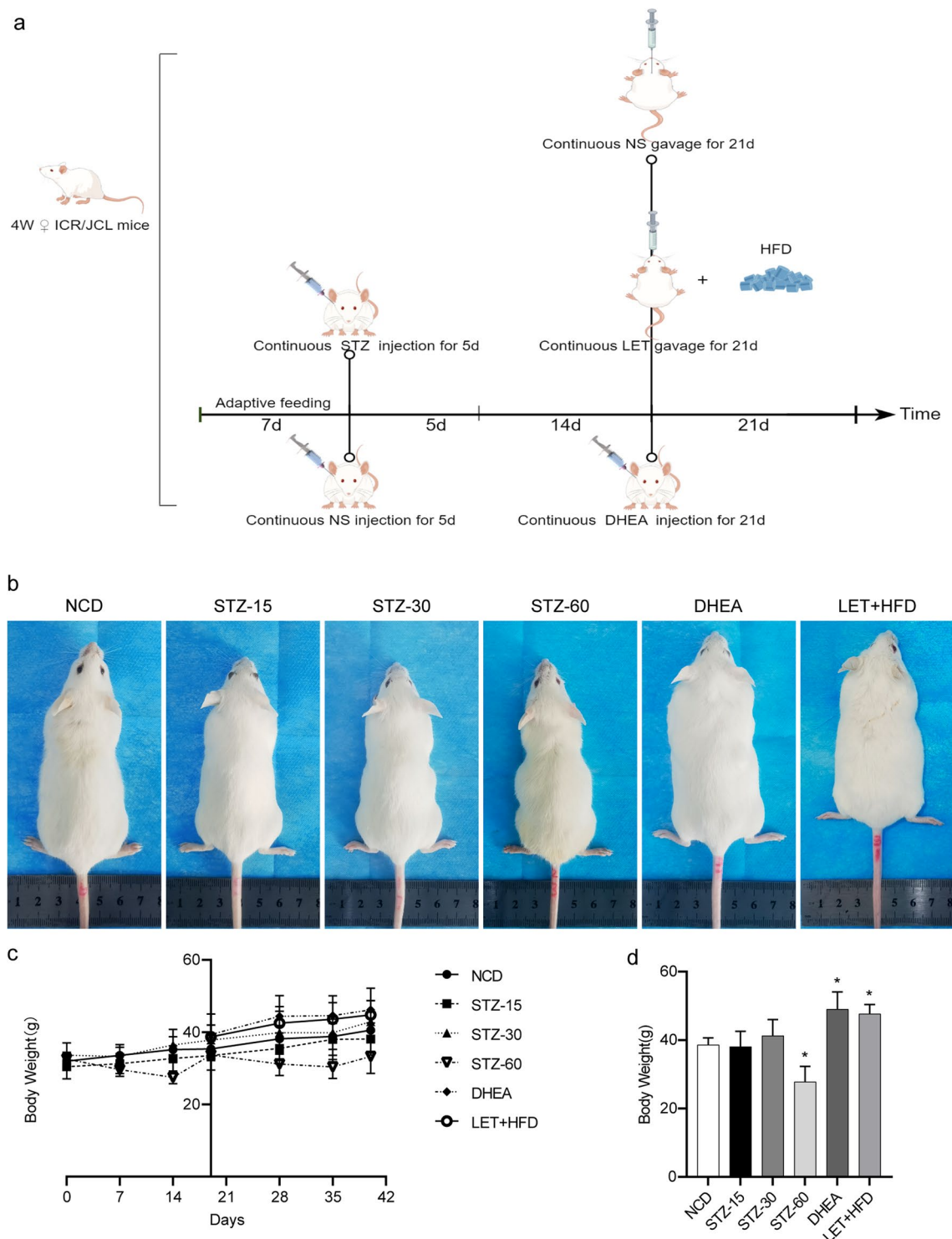


Fig. 1. STZ, DHEA and HFD + LET affect body morphology and weight of mice. **(a)** By Figuredraw; **(b)** post-molding form; **(c)** weight change throughout the experiment; **(d)** post-molding weight. *: vs. NCD, $p < 0.05$, statistically significant difference. Mean \pm standard deviation, $n = 6$.

Western blot

The expression of PI3K-AKT was detected by Western blot. The total protein of mouse ovary was collected by DNA/RNA/protein kit (omega, R6734-02), and the protein concentration was determined by BCA protein quantitative kit (China Science and Technology Biological Company). An equivalent quantity (30 mg) was separated by 10% SDS-PAGE gel electrophoresis and transferred to an immobilon-P transfer membrane (Merck & Company, Ireland, PR05505). The membrane was incubated in 5% skim milk for 1 h. The first antibody incubated overnight.

Antibody	Dilution rate	Company
β -actin	1:2000	Abcam
p-AKT	1:1000	Cell signaling
AKT	1:1000	Cell signaling
PI3K	1:1000	Affinity

Table 2. Antibodies used in WB and their dilution ratio.

Gene name	Forward/reverse	Sequences of primers
DDX4/AMH	Forward	5'-CCACACCTCTCTCCACTGGTA-3'
	Reverse	5'-GGCACAAGGTTTCAGGGGG-3'
MVH	Forward	5'-GGAACACAGCAGCAAGTGAT-3'
	Reverse	5'-TGGAGTCCTCATCCTCTGG-3'
CYP19A1	Forward	5'-AACCCGAGCCTTTGGAGAA-3'
	Reverse	5'-GGCCCGTCAGAGCTTTCA-3'
β -actin	Forward	5'-AGCCATGTACGTAGCCATCC-3'
	Reverse	5'-GCTGTGGTGAAGCTGTA-3'

Table 3. Sequences of primer.

The second antibody was incubated for 2 h. Autoradiography was then performed. The antibodies used and the dilution ratios are shown in Table 2.

Real-time PCR

To analyze gene expression, RNA was extracted from mouse ovaries using the DNA/RNA/Protein Kit, and cDNA was synthesized using the reverse transcription kit. Quantitative real-time PCR was performed using Mx3000 multiplex quantitative PCR system (SYBR). For each experimental condition, three duplicate samples were collected to determine relative expression levels. The primer sequences used in this study are as follows (Table 3).

Statistical analysis

Statistical analyses of the obtained data were performed using Prism 9.0 software. Measurement data are presented as mean \pm standard error of the mean (SEM). Two-way analysis of variance (ANOVA) was employed to compare the means of multiple samples. Body weight, fasting blood glucose, area under OGTT curve, area under ITT curve, ovarian index, follicle count, serum hormone level and RT-qPCR were all analyzed by one-way ANOVA. *P* value of <0.05 was considered to be statistically significant.

Results

STZ, DHEA and HFD + LET affect the body size and weight of mice

The changes in body weight and body morphology of mice in each group were monitored throughout the experiment. The results showed that compared with the NCD group, the STZ-60 group exhibited significant weight loss and became emaciated. The DHEA and LET + HFD groups became obese with significant increases in weight. The STZ-15 and STZ-30 groups showed no significant difference in body morphology and body weight (Fig. 1b–d).

STZ, DHEA and HFD + LET affect glucose tolerance and insulin resistance in mice

To monitor changes in blood glucose during modeling, we measured weekly random blood glucose levels across groups. The STZ-60 group showed significantly higher levels than the NCD group ($p < 0.05$, Fig. 2a). Fasting blood glucose before sampling ($p < 0.05$, Fig. 2b) revealed that all groups except DHEA had significantly higher levels than the NCD group. DHEA showed an increase but without statistical significance. The changes of glucose tolerance and insulin resistance of mice in each group were detected. OGTT ($p < 0.05$, Fig. 2e) results showed that the blood glucose level in the NCD group reached the peak at 30 min and decreased slowly at 30–120 min. Except for the DHEA group, the blood glucose level in the other groups was higher than that in the NCD group at all monitoring points. The area under the curve of OGTT of mice in each group was compared, and the glucose tolerance of mice in STZ-30, STZ-60 and LET + HFD groups was significantly impaired ($p < 0.05$, Fig. 2c). ITT results showed that the blood glucose of the NCD group reached the lowest value at 30 min and rose slowly at 30–120 min (Fig. 2f). The ITT results of each group were “normalized” (Fig. 2g) and the area under the curve was calculated (Fig. 2d). The decrease rate of blood glucose in STZ-60, DHEA and LET + HFD groups was lower than that in NCD group, and the decrease rate of blood glucose in STZ-15 group was lower than that in NCD group but close to that in NCD group, suggesting that the efficiency of insulin in promoting glucose uptake and utilization of mice in the above four groups was decreased, and there might be insulin resistance. Comparison of ITT change rate AUC (Fig. 2d) indicated that only DHEA was significantly higher than NCD

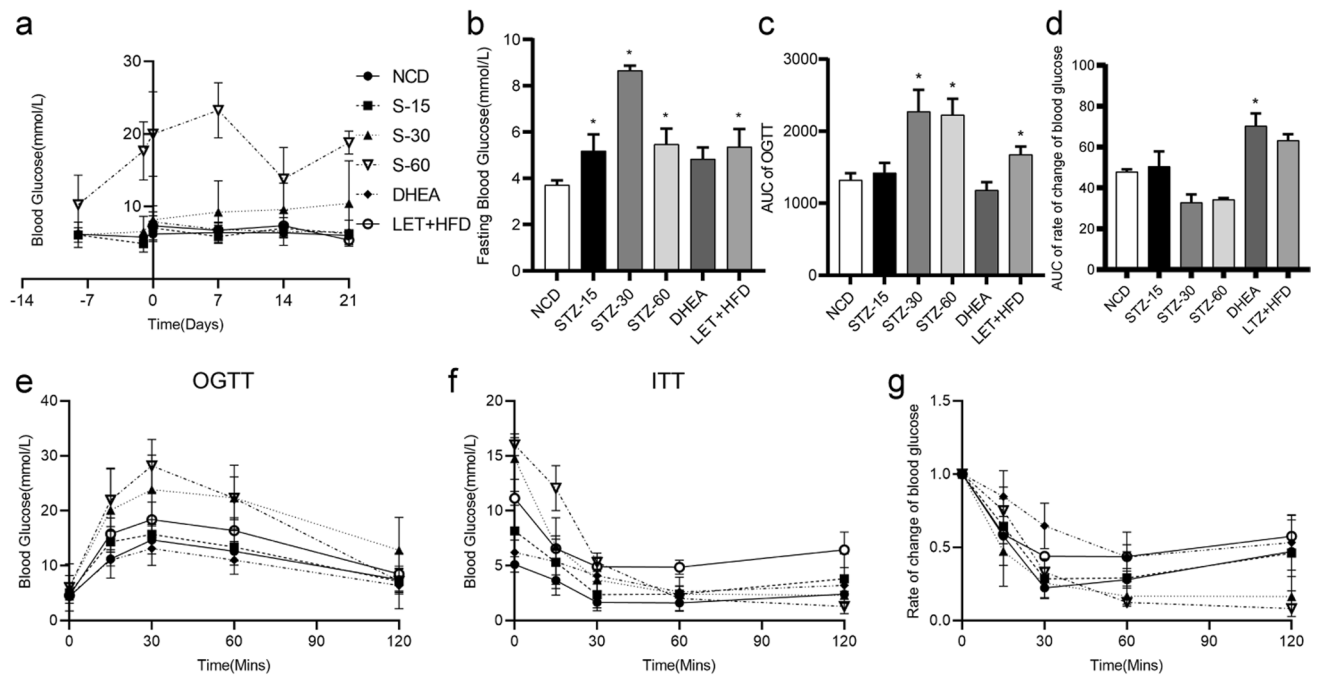


Fig. 2. Effects of STZ, DHEA and HFD + LET on glucose tolerance and insulin resistance in mice. (a) Random blood glucose changes after the start of modeling; (b) Fasting blood glucose after molding; (c) Area under OGTT curve after molding; (d) Area under the curve of figure (g); (e) OGTT after molding; (f) ITT after molding; (g) ITT change rate. *: vs. NCD, $p < 0.05$, statistically significant difference. Mean \pm standard deviation, $n = 6$.

($p < 0.05$), while the LET + HFD group was also higher but with no statistical difference, and the STZ-60 group was lower. Combined with the line chart of ITT change rate, we believed that, insulin resistance was observed in DHEA, STZ-60 and LET + HFD groups. These results showed that both STZ and LET + HFD could increase fasting blood glucose. STZ-30, STZ-60 and LET + HFD can cause abnormal glucose tolerance. STZ-60, DHEA and LET + HFD can cause insulin resistance.

STZ, DHEA and HFD + LET affect the estrous cycle of mice

After sexual maturity, female mice exhibit a periodic estrous cycle regulated by hormonal changes¹⁹. The estrous cycle reflects ovarian ovulation and endocrine function. We continuously monitored estrous cycles for 10 days prior to sampling in all groups. The NCD group exhibited a regular estrous cycle lasting approximately 4–5 days (Fig. 3a), whereas other groups displayed varying degrees of cycle disruption (Fig. 3b–f). Notably, the STZ-60 group (Fig. 3d) completely lost regular estrous cyclicity, and the LET + HFD group (Fig. 3f) remained persistently in the diestrus phase for 10 consecutive days without observable ovulation. We statistically analyzed estrous cycles across groups, the results showed that compared with the NCD group, except for the DHEA group, the estrous period was shortened and the estrous interval was prolonged in the other groups, and the LET + HFD group was continuously in the estrous interval (Fig. 3g). Mouse vaginal secretions were stained using a modified Pap test kit (Fig. 3h). Preestrus smear showed a high proportion of green nucleated epithelial cells and a low proportion of pink keratinocytes. Estrus smears exhibited a high proportion of pink keratinocytes and a low proportion of green nucleated epithelial cells. In metestrus smears, green nucleated epithelial cells, pink keratinocytes, and blue leukocytes were present at an approximate ratio of 1:1:1. Interestrus smears revealed a high number of scattered blue white blood cells and a minimal amount of mucus. Collectively, these findings demonstrate that both STZ and LET can significantly disrupt the estrous cycle. Specifically, the STZ group exhibited a shortened estrous period and prolonged estrous interval, whereas the LET group showed stagnation in the estrous interval.

Effects of STZ, DHEA and HFD + LET on ovarian size, ovarian index, ovarian morphology and percentage of follicles at all levels in mice

The mice were anesthetized by intraperitoneal injection of pentobarbital sodium (3%, 100 mg/kg) before sampling. After sampling, the appearance of the ovaries of mice in each group was photographed (Fig. 4a) and the statistical ovarian index (Fig. 4c) were recorded. Compared with NCD group, STZ-15 and STZ-30 groups exhibited increased ovarian size, STZ-60 group showed a significant reduction ($p < 0.05$), while DHEA and LET + HFD groups displayed no significant changes. Compared with the NCD group, the ovarian index of mice in the STZ-15 and STZ-30 groups increased but had no statistical difference, whereas the ovarian index of mice in STZ-60, DHEA and LET + HFD groups decreased significantly ($p < 0.05$, Fig. 4c). H&E staining of mice ovary (Fig. 4b) showed that follicles at all levels (primary follicles, secondary follicles and mature follicles) were visible in the ovaries of mice in the NCD group, and follicles at all levels were complete in structure and cell morphology

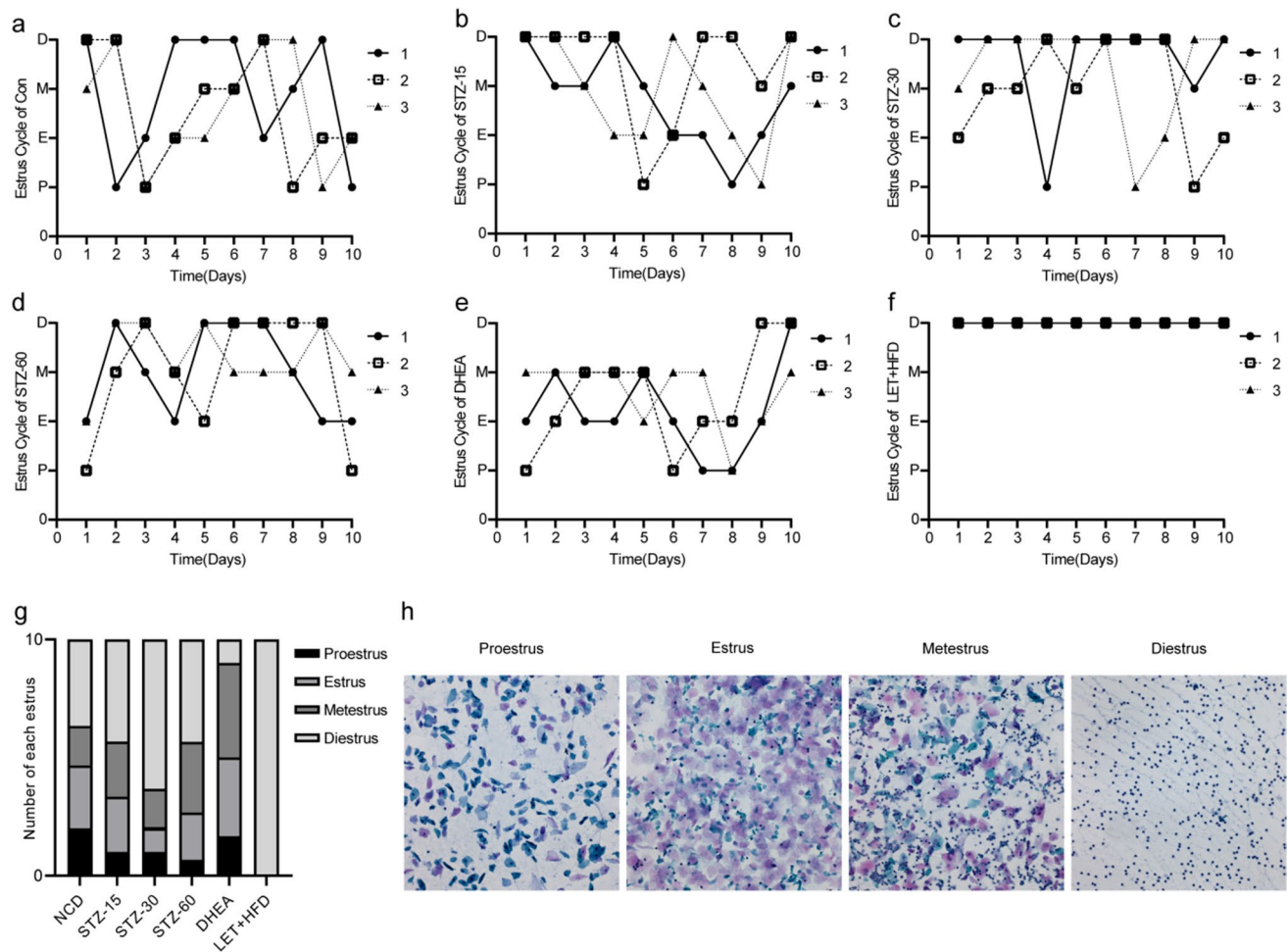


Fig. 3. STZ, DHEA, HFD + LET affect the estrous cycle of mice. (a) the estrous cycle of the NCD group; (b) The estrous cycle of STZ-15 group; (c) The estrous cycle of STZ-30 group; (d) The estrous cycle of STZ-60 group; (e) estrous cycle in DHEA group; (f) estrous cycle of LET + HFD group; (g) Histogram of the proportion of estrous cycles in each stage; (h) Pasteurization of estrous cycle smears. $n = 3-6$.

was clear. In the ovaries of mice in the STZ-15 group, STZ-30 group, STZ-60 group and DHEA group, follicles at all levels were reduced to varying degrees and corpus luteum was increased. Multiple large cystic follicles were observed in the ovaries of mice in the LET + HFD group. The granulosa cell layer in the cystic follicles became thin and contracted along the follicle wall. The follicles of mice in each group were counted and the percentages of follicles at all levels and cystic follicles in the total number of follicles were calculated (Fig. 4d). Compared with the NCD group, the percentages of primary and secondary follicles of mice in each group were decreased, however, there was no statistical difference. The percentage of mature follicles in all groups was significantly decreased, the corpus luteum in the LET + HFD group was significantly decreased, and the other groups were significantly increased ($p < 0.05$, Fig. 4d). The number of cystic follicles increased in the LET + HFD group and the difference was statistically significant ($p < 0.05$, Fig. 4d). The above results showed that STZ-60, DHEA and LET groups could reduce ovarian index, STZ, DHEA and LET could reduce mature follicles ($p < 0.05$, Fig. 4c), and LET could increase sinus follicles significantly ($p < 0.05$, Fig. 4d).

Effects of STZ, DHEA and HFD + LET on serum hormones, AMH, MVH, CYP19A1 and GnRH in mice

Serum hormone levels were measured in all groups. Compared with the NCD group, serum testosterone (TP) levels were elevated in all groups. Only the LET + HFD group exhibited a statistically significant difference ($p < 0.05$, Fig. 5a). Serum estradiol (E2) was decreased in all groups, only the STZ-15 group showed significant change ($p < 0.05$, Fig. 5b). Serum anti-Müllerian hormone (AMH) levels were elevated in all groups. Specifically, the STZ-60, DHEA, and LET + HFD groups exhibited significant increases compared to the NCD group ($p < 0.05$, Fig. 5c). Serum sex hormone-binding globulin (SHBG) levels were significantly reduced in all groups compared to the NCD group ($p < 0.05$, Fig. 5d).

The expressions of AMH, MVH, CYP19A1 and GnRH were detected by real-time PCR. Compared with the NCD group, AMH mRNA expression was elevated in the STZ-15, STZ-60, and LET + HFD groups. Statistical significance was observed in the STZ-15 and LET + HFD groups ($p < 0.05$, Fig. 5e), whereas it was decreased

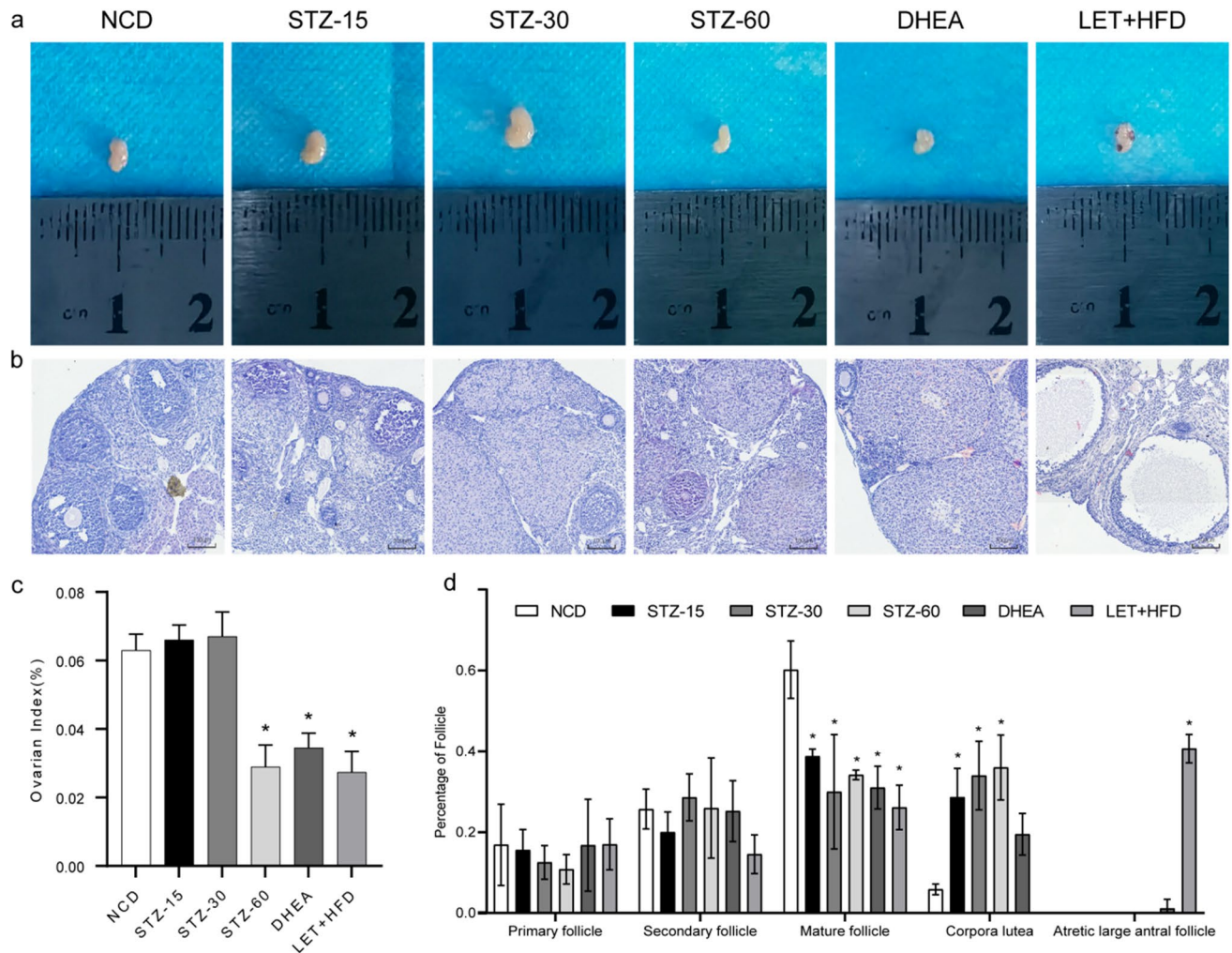


Fig. 4. Effects of STZ, DHEA and HFD + LET on ovarian size, ovarian index, ovarian morphology and percentage of follicles at all levels in mice. **(a)** Ovary of mice in each group; **(b)** H&E staining; **(c)** Ovarian index; **(d)** follicle count. *: vs. NCD, $p < 0.05$, statistically significant difference. Mean \pm standard deviation, $n = 3$.

in the remaining groups. Compared with the NCD group, MVH mRNA expression was elevated in all groups. Statistical significance was observed exclusively in the LET + HFD group ($p < 0.05$, Fig. 5f). CYP19A1 mRNA expression was elevated in the STZ-15 group but decreased in all other groups. Only the STZ-15 group exhibited a statistically significant difference (Fig. 5g). Compared with the NCD group, GnRH mRNA expression was decreased in the STZ-60 group but increased in all other groups. Statistical significance was observed exclusively in the STZ-30 and LET + HFD groups ($p < 0.05$, Fig. 5h).

STZ, DHEA and HFD + LET differentially modulated ovarian PI3K/AKT signaling pathway activation

We detected the expression of PI3K/AKT signaling pathway in the ovaries of mice across all groups. The results indicated that, compared with the NCD group, the relative expression levels of PI3K and AKT in the ovaries of mice across all groups were significantly reduced ($p < 0.05$, Fig. 6a–c).

Discussion

Female ovarian function is influenced by both genetic and environmental factors. Environmental factors can lead to dysfunction, premature ovarian failure, and even complete ovarian failure. In recent years, ovarian dysfunction induced by environmental toxins such as streptozotocin (STZ), dehydroepiandrosterone (DHEA), and letrozole (LET) combined with high-fat diet (HFD) has garnered significant attention.

STZ is an amino-glucosamine nitrosourea compound produced by some *Streptomyces achromogenes* in the soil. Potential sources of human exposure to STZ include STZ-producing bacteria, gut microbiota, animal products, etc.^{22,23}. *Streptomyces achromogenes*, a Gram-positive bacterium belonging to the genus *Streptomyces*, is widely and abundantly present in the soil^{23,24} and can flow into lakes or pollute human drinking water with rain, directly exposing humans to the STZ environment. Additionally, STZ can be enriched in animal feed,

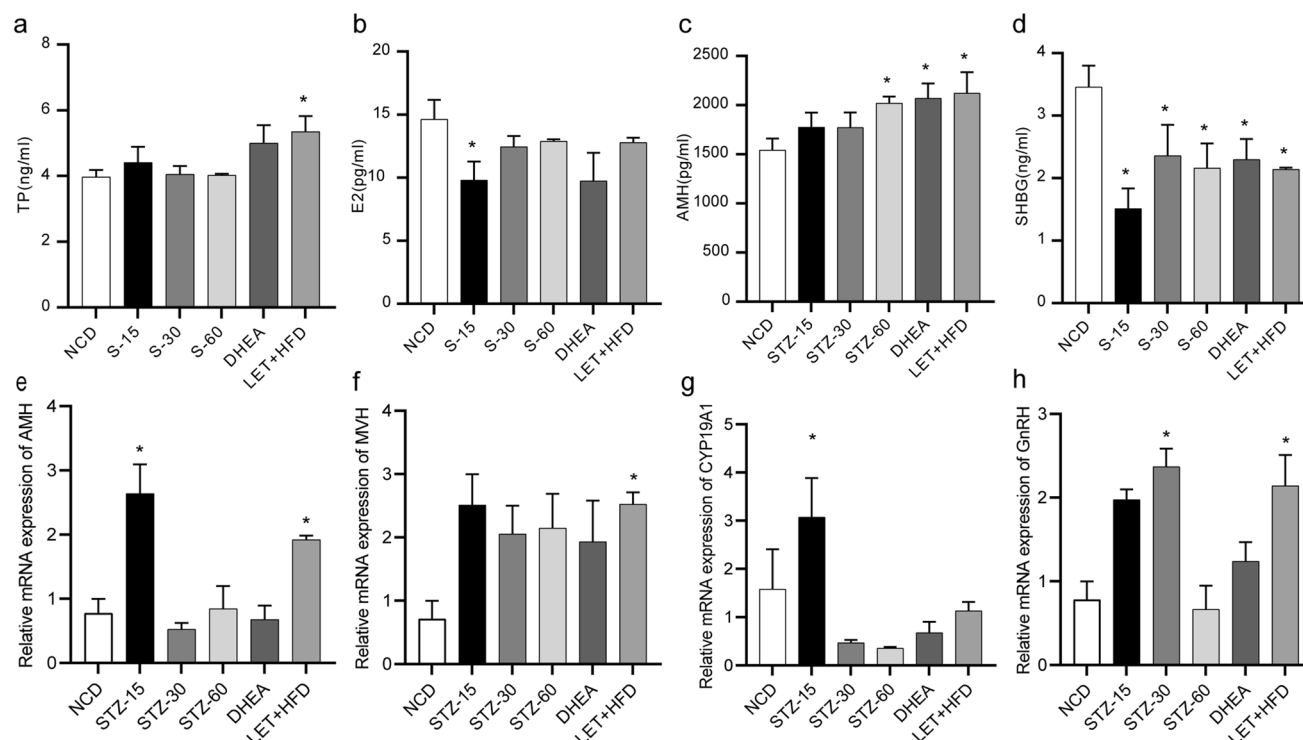


Fig. 5. Effects of STZ, DHEA and HFD + LET on serum hormones, AMH, MVH, CYP19A1 and GnRH in mice. (a) Serum testosterone (T) level of mice; (b) Serum estrogen (E2) levels in mice; (c) Mouse serum anti-Müllerian hormone (AMH); (d) Mouse serum sex hormone-binding globulin (SHBG); (e) qPCR for AMH; (f) qPCR for MVH; (g) qPCR of CYP19A1; (h) qPCR for GnRH. *: vs. NCD, $p < 0.05$, statistically significant difference. Mean \pm standard deviation, $n = 6$.

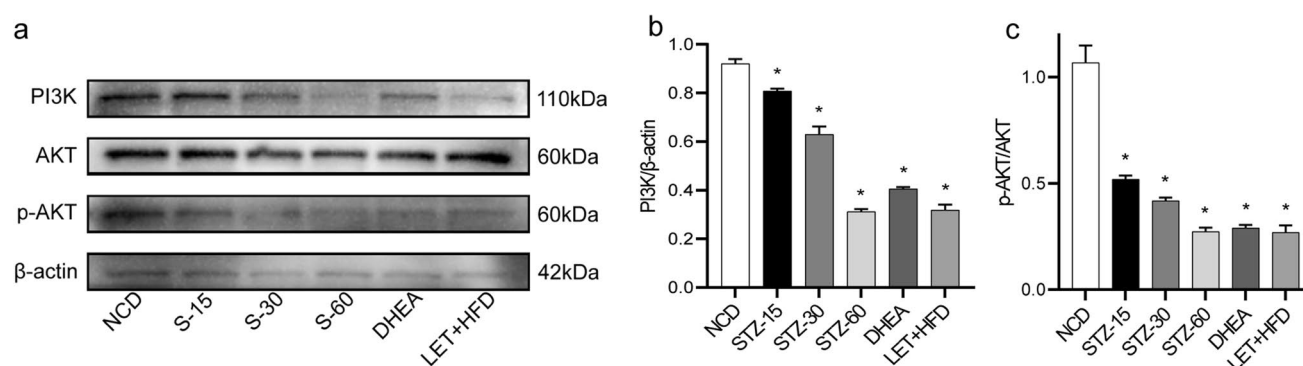


Fig. 6. STZ, DHEA, HFD + LET can affect PI3K/AKT signaling pathway in the ovary to different degrees. (a) PI3K, AKT and p-AKT Western blot, the results of western blot were obtained from two electrophoretic gels in the same bath; (b) The relative expression of PI3K protein; (c) Relative expression of p-AKT protein. *: vs. NCD, $p < 0.05$, statistically significant difference. Mean \pm standard deviation, $n = 3$.

animal products, and other organic substances through this pathway, leading to indirect accumulation in the human body. *Streptomyces* that can produce STZ has also been found in a variety of human diseases, such as skin infection and cardiopulmonary infection, etc. *Streptomyces* infection typically occurs in patients with underlying diseases that can lead to a decline in autoimmune system function. In this case, the abundance of STZ—susceptible gut microbiota in some patients increases, and the number of similar molecules of islet cell antigens produced by microorganisms increases, thereby increasing the risk of diabetes caused by STZ^{6,8}. STZ has the potential to induce diabetes in animals and has been extensively studied for its mechanisms and effects^{23,25}. In rodent studies, multiple low-dose intraperitoneal injection of STZ did not cause an increase in mouse body weight. In our experiment, we found that low-dose STZ (15 and 30 mg/kg/day) did not significantly affect mouse body weight, whereas 60 mg/kg/day STZ induced significant weight loss²⁵. Additionally, as a cytotoxic drug to animal islet β cells, STZ can damage islet β cells through free radicals, impair insulin synthesis,

reduce insulin content, leading to glucose metabolism disorders. It has been reported that 60 mg/kg/day of STZ can induce obvious insulin resistance in mice^{6,18,25}, and our study confirmed the same result. Additionally, our experiment revealed that both 15 mg/kg/day and 30 mg/kg/day of STZ induced abnormal fasting blood glucose levels in mice; whereas 30 mg/kg/day and 60 mg/kg/day of STZ caused abnormal glucose tolerance. Notably, STZ at 15 mg/kg/day did not show significant changes.

DHEA is an endogenous hormone, which is mainly produced by the adrenal cortex zona reticularis in the human body and is crucial for the synthesis of testosterone and dihydrotestosterone^{8,9,11,26}. There are various ways of exogenous exposure to DHEA. Reports indicate that DHEA enhances anabolic effects, reduces muscle tension during athletic competitions and training, and accelerates physical recovery. It is now listed as a banned substance in competitions by the International Olympic Committee²⁷. In the livestock industry, steroids such as DHEA are commonly used as growth promoters to promote the feed conversion rate of livestock, promote the growth and development, synchronous estrus, and increase the body weight of animals, thereby improving the economic benefits of livestock^{28,29}. Specifically, androgen promote protein synthesis and basal metabolism in animals. Progesterone can enhance the appetite of animals and improve the feed conversion rate, and estrogen is often used as a growth promoter and estrus inducer. Even after metabolism in animal bodies, steroid hormones remain detectable in animal-derived foods. Their nature and quantity of remain unchanged despite freezing or heating, enriching them in the human body through the food chain¹. Although primarily produced in humans, some studies suggest that DHEA and its metabolites may be present in the environment, entering it via various pathways including human and animal excreta and industrial emissions. However, the DHEA level in the environment is usually low, and its impact on the environment and human health requires further study. Some studies have pointed out that increasing the DHEA level in the human body through exogenous pathways leads to an increase in androgen levels and disrupts the maturation and ovulation of oocytes, which is related to the occurrence of polycystic ovary syndrome (PCOS)^{3,10,26}. In addition, DHEA also has a variety of biological activities. In theca cells, it may promote the production of dihydrotestosterone (DHT) and testosterone (T) through the $\Delta 5$ pathway and increase the serum testosterone (TP) level^{30,31}. Many reports have pointed out that the accumulation of DHEA in the body will affect the normal function of the hypothalamic–pituitary–ovarian axis through LH, causing model animals to exhibit various reproductive phenotypes similar to human PCOS, such as increased androgen levels, disordered estrous cycle, and polycystic ovaries^{31–33}. In many studies on DHEA, it has been pointed out that DHEA can cause an increase in the body weight of the model group^{19,26,34}, which is consistent with our findings. In addition, in our study, it was found that the DHEA group showed insulin resistance, but there was no obvious abnormal fasting blood glucose and glucose tolerance, which is consistent with the research of Furat et al.^{26,31,34}.

Letrozole is a synthetic new type of highly selective aromatase inhibitor, which inhibit the conversion of androgen to estrogen, leading to androgen accumulation and estrogen reduction. It is commonly used in the treatment of breast cancer¹⁹. In addition, an appropriate dose of letrozole can also promote ovulation. Letrozole is a widely used drug. Although its specific use and emission situation are not detailed in the provided search results, improper use or disposal of the drug and the excretion of patients can discharge the residual letrozole into sewage, and letrozole can then enter the water body and has the risk of being enriched in the soil³⁵. In addition, LET has been reported to affect ovarian function³⁶. High-fat diet (HFD), a model of unhealthy dietary habits, is associated with obesity, insulin resistance, hormonal dysregulation, and ovarian dysfunction³⁷. In our experiment, we observed that the combination of LET and HFD induced obesity, polycystic ovaries, hyperandrogenemia, impaired glucose tolerance, and insulin resistance in mice, consistent with findings by Peng et al.¹⁹. This study did not involve a group solely treated with HFD, as it primarily induces metabolic syndrome rather than a typical PCOS phenotype. Future work will design controlled experiments to specifically investigate the independent mechanisms of HFD in the ovarian microenvironment.

Under normal circumstances, in the ovarian theca cells and adrenal cortex of women, precursor cholesterol is converted into testosterone through a series of reactions, and then testosterone is transferred to the granulosa cells and converted into estrogen. In this process, follicle—stimulating hormone (FSH) can regulate the synthesis of cytochrome p450 aromatase and the conversion of androgen to estrogen in granulosa cells, and luteinizing hormone (LH) regulates the synthesis of androgen in theca cells and reduces the level of sex hormone—binding globulin (SHBG), resulting in an increase in the concentration of free androgen and a hyperandrogenic state^{19,38}. Anti-mullerian hormone (AMH) can reflect the ovarian reserve function of women. In women, AMH inhibits the recruitment of primary follicles and may inhibit the action of FSH, leading to ovulation disturbance³⁸. The results of our experiment showed that, except for the STZ-60 group, the other groups could increase the serum TP level of mice, and the LET + HFD group had a statistically significant increase; the above groups could all increase the serum AMH level, and the STZ-60, DHEA, and LET + HFD groups had statistically significant increases, and the LET + HFD group caused a higher increase in the serum TP and AMH levels than the other groups. It has been reported that the accumulation of STZ in the body can induce a lean non-diabetic PCOS mouse model in C57BL/J6 mice. However, in our experiment, the results of follicle counting showed that in the STZ-15, STZ-30, and STZ-60 groups, the number of follicles at all levels decreased, and the decrease in mature follicles was the most obvious, but there was no obvious hyperandrogenemia and polycystic ovary changes.

The PI3K/AKT signaling pathway is a critical intracellular pathway that plays a pivotal role in cellular growth, proliferation, and metabolism³⁹. AKT (also known as protein kinase B) is a direct downstream target protein of PI3K^{40,41}. The PI3K/AKT signaling pathway not only plays an essential role in regulating glucose metabolism and insulin resistance (IR)⁴², but also influences granulosa cell proliferation and apoptosis. The suppression of granulosa cell proliferation is considered a key factor contributing to the abnormal follicular development observed in polycystic ovary syndrome (PCOS)^{41,43}. In our study, p-AKT levels were significantly downregulated across all experimental groups, a finding consistent with the results reported by Min Wang et al.⁴⁴. In a study

Group	STZ-15	STZ-30	STZ-60	DHEA	LET + HFD
Obesity				√	√
Impaired fasting glucose	√	√	√		√
Abnormal glucose tolerance		√	√		√
Insulin resistance			√	√	√
Disturbed estrous cycle	√	√	√		√
Oligovulation or no ovulation	√	√	√	√	√
Cystic follicles					√
Decreased ovarian index			√	√	√
Hyperandrogenism					√
Increased serum AMH			√	√	√
Decreased serum estrogen	√				
Decreased serum sex hormone binding globulin	√	√	√	√	√

Table 4. Effects of STZ, DHEA and HFD + LET on mouse phenotypes.

by Xiaojing Zhang et al., reduced PI3K expression was observed in mouse ovaries exhibiting polycystic ovarian morphology, ovulatory dysfunction, hyperandrogenism, and IR⁴¹, which aligns with our findings.

Conclusion

This paper provides a detailed description of the scientific background regarding the impact of environmental factors, such as STZ, DHEA, and LET combined with HFD, on ovarian function. Based on the experimental design and preliminary results, we found that different doses of STZ could cause oligovulation/anovulation, abnormal fasting blood glucose, without obesity, with or without abnormal glucose tolerance in mice. The administration of DHEA in mice resulted in oligovulation/anovulation with obesity, some cystic follicles, and an insignificant increase in androgen. Administration of LET + HFD in mice resulted in dilute oligovulation/anovulation, cystic follicles, and hyperandrogenemia, with obesity, abnormal fasting blood glucose, abnormal glucose tolerance, and insignificant insulin resistance (Table 4). Our study not only enriches the theoretical framework regarding the relationship between environmental factors and ovarian health but also provides new insights into the prevention and treatment of ovarian dysfunction caused by environmental factors. Future studies should further explore the specific molecular mechanisms of environmental factors affecting ovarian function, so as to provide scientific basis for formulating effective intervention strategies.

Data availability

Data is provided within the manuscript. The current study dataset is available upon reasonable request from corresponding author Ruihe. Email address: Ruihe515@163.com. We have provided the above information in the manuscript (Line 649–650).

Received: 29 September 2024; Accepted: 12 September 2025
Published online: 08 October 2025

References

1. Chaomin, Z. *Technological Study of Detection and Identification of Endogenous and Exogenous Hormone Residues in Foodstuffs of Animal Origin* (SCUT (South China University of Technology), 2014).

2. De Luca, M. et al. Interaction of letrozole and its degradation products with aromatase: Chemometric assessment of kinetics and structure-based binding validation. *J. Enzyme Inhib. Med. Chem.* **37**(1), 1600–1609 (2022).

3. Liao, B. et al. Effects of androgen excess-related metabolic disturbances on granulosa cell function and follicular development. *Front. Endocrinol. (Lausanne)* **13**, 815968 (2022).

4. Chung, H. S. et al. Uptake of the veterinary antibiotics chlortetracycline, enrofloxacin, and sulphathiazole from soil by radish. *Sci. Total Environ.* **605–606**, 322–331 (2017).

5. Srivastava, S., Pandey, H. & Tripathi, Y. B. Expression kinetics reveal the self-adaptive role of beta cells during the progression of diabetes. *Biomed. Pharmacother.* **106**, 472–482 (2018).

6. Furman, B. L. Streptozotocin-induced diabetic models in mice and rats. *Curr. Protoc.* **1**(4), e78 (2021).

7. Wang, L. J. et al. Dehydroepiandrosterone sulfate, free testosterone, and sex hormone-binding globulin on susceptibility to attention-deficit/hyperactivity disorder. *Psychoneuroendocrinology* **103**, 212–218 (2019).

8. Zdrojewicz, Z. & Kesik, S. Dehydroepiandrosterone (DHEA)—youth hormone?. *Wiad. Lek.* **54**(11–12), 693–704 (2001).

9. Rutkowski, K. et al. Dehydroepiandrosterone (DHEA): Hypes and hopes. *Drugs* **74**(11), 1195–1207 (2014).

10. Zhang, Y. & Xu, L. Comparative study of DHEA and letrozole induced polycystic ovary syndrome in post-pubertal rats. *Gynecol. Endocrinol.* **38**(5), 425–431 (2022).

11. Friess, E. et al. Dehydroepiandrosterone—A neurosteroid. *Eur. J. Clin. Invest.* **30**(Suppl 3), 46–50 (2000).

12. Burger, H. G. Androgen production in women. *Fertil. Steril.* **77**(Suppl 4), S3–S5 (2002).

13. Yang, Q., Wan, Q. & Wang, Z. Curcumin mitigates polycystic ovary syndrome in mice by suppressing TLR4/MyD88/NF-kappaB signaling pathway activation and reducing intestinal mucosal permeability. *Sci. Rep.* **14**(1), 29848 (2024).

14. Johnson, P. E. & Buzdar, A. Are differences in the available aromatase inhibitors and inactivators significant?. *Clin. Cancer Res.* **7**(12 Suppl), 4360s–4368s (2001).

15. Hu, R. et al. Characteristics of polycystic ovary syndrome rat models induced by letrozole, testosterone propionate and high-fat diets. *Reprod. Biomed. Online* **50**(1), 104296 (2024).

16. Liu, X. L. Research advances in animal models of polycystic ovary syndrome. *J. Qingdao Univ. (Med. Sci.)* **60**(05), 787–790 (2024).

17. Hu, R. et al. Characteristics of polycystic ovary syndrome rat models induced by letrozole, testosterone propionate and high-fat diets. *Reprod. Biomed. Online* **50**(1), 104296 (2025).
18. Ryu, Y. et al. Consecutive low doses of streptozotocin induce polycystic ovary syndrome features in mice. *Int. J. Mol. Sci.* **22**(3), 1299 (2021).
19. Peng, Q. et al. Metformin improves polycystic ovary syndrome in mice by inhibiting ovarian ferroptosis. *Front. Endocrinol. (Lausanne)* **14**, 1070264 (2023).
20. Liang, X. et al. Study on the effects and mechanisms of Wenzhong Bushen Formula in improving ovarian reserve decline in mice based on network pharmacology. *J. Ethnopharmacol.* **324**, 117756 (2024).
21. Myers, M. et al. Methods for quantifying follicular numbers within the mouse ovary. *Reproduction* **127**(5), 569–580 (2004).
22. Zhu, B. T. Pathogenic mechanism of autoimmune diabetes mellitus in humans: Potential role of streptozotocin-induced selective autoimmunity against human islet beta-cells. *Cells* **11**(3), 492 (2022).
23. Grieb, P. Intracerebroventricular streptozotocin injections as a model of Alzheimer's disease: In search of a relevant mechanism. *Mol. Neurobiol.* **53**(3), 1741–1752 (2016).
24. Zhang, Y. et al. Remediation of sulfathiazole contaminated soil by peroxymonosulfate: Performance, mechanism and phytotoxicity. *Sci. Total Environ.* **830**, 154839 (2022).
25. Kamli-Salino, S. et al. Induction of experimental diabetes and diabetic nephropathy using anomer-equilibrated streptozotocin in male C57Bl/6J mice. *Biochem. Biophys. Res. Commun.* **650**, 109–116 (2023).
26. Wu, H. et al. Dehydroepiandrosterone-induced polycystic ovary syndrome mouse model requires continuous treatments to maintain reproductive phenotypes. *J. Ovarian Res.* **16**(1), 207 (2023).
27. Min, S. et al. Study on the metabolism of exogenous DHEA and its metabolites level. *Chin. J. Med. Expertise* **3**, 19–22 (2007).
28. Kanimozhi, S. et al. Investigation of bioaccumulation profile of oestrogens in zebrafish liver by hollow fibre protected liquid phase microextraction with gas chromatography-mass spectrometric detection. *J. Chromatogr. B Anal. Technol. Biomed. Life Sci.* **909**, 37–41 (2012).
29. Kuuranne, T. et al. Electrospray and atmospheric pressure chemical ionization tandem mass spectrometric behavior of eight anabolic steroid glucuronides. *J. Am. Soc. Mass Spectrom.* **11**(8), 722–730 (2000).
30. Kafali, H. et al. Letrozole-induced polycystic ovaries in the rat: A new model for cystic ovarian disease. *Arch. Med. Res.* **35**(2), 103–108 (2004).
31. Wang, X. et al. Effects of dehydroepiandrosterone alone or in combination with a high-fat diet and antibiotic cocktail on the heterogeneous phenotypes of PCOS mouse models by regulating gut microbiota. *Front. Endocrinol. (Lausanne)* **13**, 1030151 (2022).
32. Wu, Y. X. et al. Naringenin regulates gut microbiota and SIRT1/PGC-1 α signaling pathway in rats with letrozole-induced polycystic ovary syndrome. *Biomed. Pharmacother.* **153**, 113286 (2022).
33. Kim, E. J. et al. An Improved dehydroepiandrosterone-induced rat model of polycystic ovary syndrome (PCOS): post-pubertal Improve PCOS's features. *Front. Endocrinol. (Lausanne)* **9**, 735 (2018).
34. Furat, R. S. et al. Effect of resveratrol and metformin on ovarian reserve and ultrastructure in PCOS: an experimental study. *J. Ovarian Res.* **11**(1), 55 (2018).
35. Liao, P. H. et al. Persistent endocrine disruption effects in medaka fish with early life-stage exposure to a triazole-containing aromatase inhibitor (letrozole). *J. Hazard. Mater.* **277**, 141–149 (2014).
36. Goswami, S. K. et al. A randomized single-blind controlled trial of letrozole as a low-cost IVF protocol in women with poor ovarian response: A preliminary report. *Hum. Reprod.* **19**(9), 2031–2035 (2004).
37. Jiang, Y. et al. Cellular atlases of ovarian microenvironment alterations by diet and genetically-induced obesity. *Sci. China Life Sci.* **67**(1), 51–66 (2024).
38. Rudnicka, E. et al. Anti-mullerian hormone in pathogenesis, diagnostic and treatment of PCOS. *Int. J. Mol. Sci.* **22**(22), 12507 (2021).
39. Tong, C. et al. Insulin resistance, autophagy and apoptosis in patients with polycystic ovary syndrome: Association with PI3K signaling pathway. *Front. Endocrinol. (Lausanne)* **13**, 1091147 (2022).
40. Brown, A. E. & Walker, M. Genetics of insulin resistance and the metabolic syndrome. *Curr. Cardiol. Rep.* **18**(8), 75 (2016).
41. Zhang, X. et al. Study on the mechanism of action of berberine combined with Jianpi Yishen Huazhuo formulation in treating obese polycystic ovary syndrome by activating PI3K/AKT signaling pathway. *Gynecol. Endocrinol.* **41**(1), 2462068 (2025).
42. Cheung, Y. M., McDonnell, M. & Hamnvik, O. R. A targeted approach to phosphoinositide-3-kinase/Akt/mammalian target of rapamycin-induced hyperglycemia. *Curr. Probl. Cancer* **46**(1), 100776 (2022).
43. Gong, Y. et al. Growth hormone activates PI3K/Akt signaling and inhibits ROS accumulation and apoptosis in granulosa cells of patients with polycystic ovary syndrome. *Reprod. Biol. Endocrinol.* **18**(1), 121 (2020).
44. Wang, M. et al. The role of CLDN11 in promotion of granulosa cell proliferation in polycystic ovary syndrome via activation of the PI3K-AKT signalling pathway. *Sci. Rep.* **15**(1), 3533 (2025).

Acknowledgements

This paper is supported by Ningxia Natural Science Foundation (2022AAC02033), Ningxia Key Research and Development Project (2022BEG02034, 2021BEB04034), National Natural Science Foundation of China (82460172).

Author contributions

Leyi Yu: Writing—original draft, validation, software, methodology, formal analysis. Qingjie Peng: Validation, methodology, formal analysis. Cunling Ma: Visualization, formal analysis. Jiahui Ouyang: Writing—original draft. Hongru Ma: Validation, formal analysis. Shuzhe Fan: Methodology. Miao Sun: Visualization. Huiming Ma: Validation. Xiaoli Du: Supervision, methodology. Xiangdong Zhu: Supervision, resources, methodology. Guangyong Li: Supervision, methodology. Rui He: Writing—review and editing, supervision, resources, methodology.

Declarations

Competing interests

The authors declare no competing interests.

Ethics approval and consent to participate

All experimental procedures were performed in accordance with the guidelines of the Institutional Animal Care and Use Committee of Ningxia Medical University and ethical approval was obtained for the animal

experiments conducted in the study (Certificate number: 10752309202000082), following the guidelines of the US National Institutes of Health and the Animal Research Reporting In Vivo Experiments (ARRIVE).

Additional information

Supplementary Information The online version contains supplementary material available at <https://doi.org/10.1038/s41598-025-20174-8>.

Correspondence and requests for materials should be addressed to X.D., X.Z., G.L. or R.H.

Reprints and permissions information is available at www.nature.com/reprints.

Publisher's note Springer Nature remains neutral with regard to jurisdictional claims in published maps and institutional affiliations.

Open Access This article is licensed under a Creative Commons Attribution-NonCommercial-NoDerivatives 4.0 International License, which permits any non-commercial use, sharing, distribution and reproduction in any medium or format, as long as you give appropriate credit to the original author(s) and the source, provide a link to the Creative Commons licence, and indicate if you modified the licensed material. You do not have permission under this licence to share adapted material derived from this article or parts of it. The images or other third party material in this article are included in the article's Creative Commons licence, unless indicated otherwise in a credit line to the material. If material is not included in the article's Creative Commons licence and your intended use is not permitted by statutory regulation or exceeds the permitted use, you will need to obtain permission directly from the copyright holder. To view a copy of this licence, visit <http://creativecommons.org/licenses/by-nc-nd/4.0/>.

© The Author(s) 2025